Desalination and Water Treatment
www.deswater.com
29 (2011) 241–251
May
1944-3994 / 1944-3986 © 2011 Desalination Publications. All rights reserved.
doi: 10.5004/dwt.2011.1739

Kinetic studies and equilibrium isotherm analyses for the adsorption of Methyl Orange by coal fly ash from aqueous solution

Manickam Matheswaran

Department of Chemical Engineering, National Institute of Technology, Tiruchirappalli – 620 015, Tamilnadu, India
Tel. +91 4144-230797; email: math_chem95@rediffmail.com

Received 29 December 2009; Accepted in revised form 15 December 2010

ABSTRACT

The coal fly ash waste generated from thermal power plant has been used as low cost adsorbent for the removal of methyl orange (MO) from the aqueous solution. In the batch experiments, the effect of various parameters was studied such as contact time, pH, adsorbent dosage, dye concentration and temperature. The adsorption of MO on the fly ash at different temperatures follows the pseudo second order kinetics. Freundlich, Langmuir, Redlich–Peterson (R–P), Temkin and Dubnin–Radushkevich isotherm models using nonlinear regression technique for the adsorption of MO were analyzed. R–P and Langmuir isotherms were found to be suitable to represent the data for adsorption. Error analysis shows that the Langmuir isotherm best fits the adsorption data at various temperatures. Isotherms have also been used to obtain thermodynamic parameters such as free energy, enthalpy and entropy. The adsorption of MO was exothermic in nature (ΔH: –38.16 to –36.41 kJmol^{-1}) with increasing temperature over range of 303–333 K.

Keywords: Methyl orange; Fly ash; Adsorption; Kinetics; Isotherms; Thermodynamic parameters

1. Introduction

Textile industries using large amount of dyes, inorganic compounds, detergents, finishing and bleaching agents increase the dissolved solids concentration in wastewater and discharge of the effluent in to rivers and lakes. The dyes effluent is toxic to the aquatic life and causes damage to the aesthetic nature of the environment. Color is recognized as one of the contaminants because it is visible to the human eye [1]. Many countries have made environmental regulations to decolorize the dye wastewater before discharging [2]. Therefore, it is required to treat the effluent for removal of dye in an economical fashion and to obtain the prescribed concentration levels before discharging into the environment. The textile effluent is treated by many physical and chemical methods including adsorption [3,4], coagulation [5], precipitation, ultrafiltration [6], electrochemical [7], and filtration with coagulation [8]. However, all the above methods suffered with some limitations and none of these completely removed color from the wastewater.

The adsorption process is one of the most efficient methods for the removal of organic and inorganic pollutants from aqueous phase and also an alternative treatment, if especially the adsorbent is inexpensive and readily available [6]. This process is attributed to its low cost, simplicity of design, high efficiency, easy availability and ability to treat high concentration of dye effluent.

Activated carbon is widely used as an adsorbent for the removal of organic matter because it has a high

* Corresponding author.

adsorption capacity, but its usage is limited because of high cost. Therefore in recent years many researchers has been devoted to study the different types of low cost and ideal adsorbents for the adsorption of organic compounds from thermal and sugar industrial waste. Coal [9], fly ash [10,11], wood [12], silica [13], clay materials [14], agricultural wastes (bagasse pith, maize cob, coconut shell, rice husk, etc.) and cotton wastes have been tried as an absorbent for color removal [10,15–18]. Adsorption and various anaerobic treatment processes for the treatment of textile effluents were reported in the review articles by Lambert and Graham [19] and Delee et al. [20]. However, some of these adsorbents have problems associated with regeneration and recovery of useful materials, which made them unattractive for wider commercial applications.

The aim of this work is to investigate the equilibrium and kinetics parameters for the basic dye of MO adsorption using fly ash. A comparison of linear least-squares and non-linear method of isotherms, Langmuir, Freundlich, Redlich–Peterson (R–P), Temkin and Dubnin–Radushkevich (D–R) was done under different temperatures. Error analysis was carried out to test the adequacy and accuracy of the model equations. Effects of different parameters such as pH, MO concentration, temperature, fly ash dosage were also studied to find optimum operating conditions. Thermodynamics parameters like the change in Gibbs free energy, enthalpy and entropy of adsorption were calculated.

2. Experimental

2.1. Materials and methods

Analytical grade chemicals are used in this experiment. MO dye [formula weight: $C_{14}H_{14}N_3NaO_3S$; molecular weight: 327.34. C.I. no. 13025, λ_{max}: 464 nm] was supplied by Merck. The structure of this dye is shown in Fig. 1. An accurately weighed quantity of the dye was dissolved in double distilled water to prepare stock solution (1000 mgL^{-1}). Experimental solutions of desired concentration were obtained by successive dilutions with double distilled water. The pH of the solutions was adjusted using reagent grade dilute sulfuric acid (0.1 N) and sodium hydroxide (0.1 N).

The coal fly ash sample was obtained from thermal power station of Neyveli Lignite Corporation, Tamilnadu, India. The fly ash was sieved to the desired mesh size range –16 to +30 meshes and washed with distilled water for removing the dissolved matter and dried at 373 K for 24 h and then kept in vacuum desiccators. The chemical composition of fly ash is given in Table 1. The surface area and the specific gravity were 1260 m^2g^{-1} and 1.33 gcm^{-3} respectively as characterized [21].

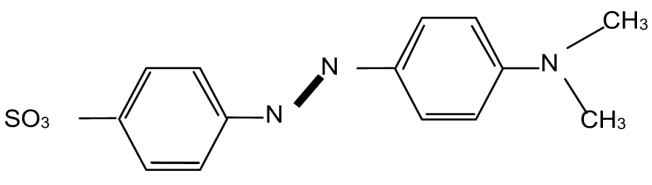

Fig. 1. Structure of Methyl Orange.

Table 1
Chemical composition of fly ash derived from lignite coal

Component	%
SiO_2	41.7
CaO	22.5
Al_2O_3	17.1
Fe_2O_3	6.63
MgO	4.91
P_2O_5	3.83
Na_2O	1.38
SO_3	0.42
K_2O	0.4
LOI*	1.13

* Loss on ignition indicates the carbon content

2.2. Analysis of the samples

The concentrations of the dye in the sample solution were measured in a Genesys-2 spectrophotometer (Thermo Spectronic, USA). All measurements were performed at the wavelength of 464 nm using distilled water as the blank.

2.3. Adsorption experiments

Adsorption experiments were conducted in a batch mode using aqueous solution of MO. Batch sorption studies were performed at different pH, temperature, initial concentration of MO and adsorbent dosage to obtain equilibrium condition and isotherms data which is required for design. A stock solution of MO with a concentration of 1000 mgL^{-1} was prepared in the distilled water. From the stock solution, various concentrations were prepared by dilution. 200 mL solution of MO with the concentration range of 200–1000 mgL^{-1} was taken in a 250 mL conical flask containing measured quantities of fly ash (100–800 mg) and was adjusted to the desired pH. The samples were shaken in a thermostatic mechanical shaker for the desired time periods, up to a maximum of 8 h, at the constant temperature, pH and a shaking speed of 200 strokes/min. The contact time and other conditions were selected on the basis of preliminary experiments, which demonstrated that the equilibrium was established in 5–6 h. Therefore, a contact period of 6 h was finally selected for all of the equilibrium tests.

The samples were separated from the adsorbent by centrifugation and were filtered using Whatman No. 42 filter paper. The residual concentration of MO is determined by UV-Vis spectrophotometer at the corresponding λmax. All the measurements were carried out at room temperature. The effect of pH for the adsorption of MO was studied by changing solution's pH over the range of 1–10. Adsorption isotherms were obtained by the fly ash dosage of 500 mgL^{-1} with solution concentration of MO (200–1000 mgL^{-1}) at different temperatures (303–333 K).

The dye concentration retained in the adsorbent phase was calculated according to Eq. (1)

$$q_e = \left(\frac{C_0 - C_e}{W}\right) - V \quad (1)$$

where C_o and C_e are the initial and equilibrium concentrations (mgL^{-1}) of dye in aqueous solution respectively, V is the volume (L), and W is the weight (mg) of the adsorbent.

3. Results and discussion

3.1. Effect of initial pH

The effect of solution's initial pH on the adsorption of initial MO concentration 500 mgL^{-1} by the amount of fly ash (500 mgL^{-1}) at a temperature of 303 K is shown in Fig. 2. Experiments were performed using various initial pH's varying from 1 to 10. The percentage removal of MO on the fly ash was above 96% and slightly decreased with increasing pH up to 4. Upon a further increase in pH (>4), the percentage adsorption was sharply decreased with increasing pH and at pH 10 the adsorption was found to be a minimum. Further, the subsequent adsorption experiments were carried out in an acidic range and pH 4 was selected as the optimum condition. Similar trend of result was observed by Wu et al. [22].

3.2. Effect of adsorbent dosage

The effects of adsorbent dosage on the percentage removal of MO by fly ash at initial concentration of MO 500 mgL^{-1}, pH 4 and temperature 303 K is shown in Fig. 3. It can be seen that the percentage removal of MO increases up to a certain limit and then it remains almost constant. The adsorption of MO was increasing with the adsorbent dosage which can be attributed to large surface area and to the availability of more adsorption sites. For adsorbent dosage greater than 500 mgL^{-1}, the incremental MO removal becomes very low, as the surface MO concentration and the solution MO concentration comes to equilibrium with each other. When the amount of adsorbent is greater than 500 mgL^{-1}, the removal efficiency becomes almost constant. All further experiments were carried out at an optimum amount of 500 mgL^{-1} adsorbent dosage.

3.3. Effect of initial concentration

Fig. 4 shows the effect of initial concentration on the percentage removal of MO and equilibrium concentration in the adsorbent phase by fly ash. The amount of adsorbed was increased per unit mass of adsorbent and the percentage of MO removal was decreased with the increasing of initial concentration. As initial concentrations were increased from 200 to 1000 mgL^{-1}, the adsorption capacity of MO on the fly ash increased from 78 to 374 mgg^{-1}. The initial concentration provided the necessary driving force to overcome the mass transfer of MO resistances between

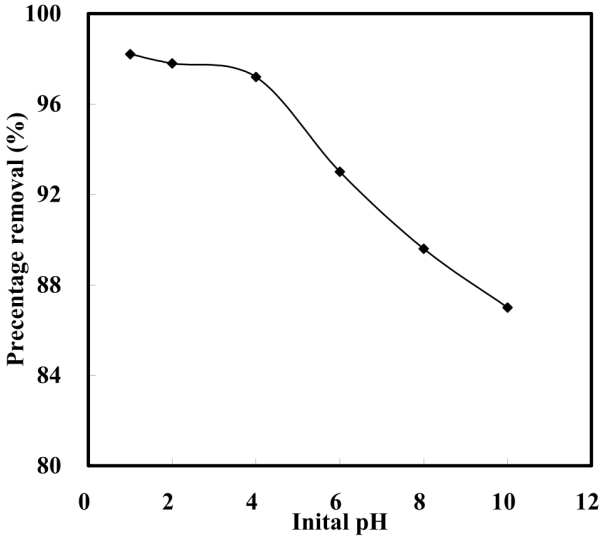

Fig. 2. Effect of initial pH on the percentage removal of MO by fly ash ([MO] = fly ash dosage = 500 mgL^{-1}, temperature = 303 K, t = 6 h).

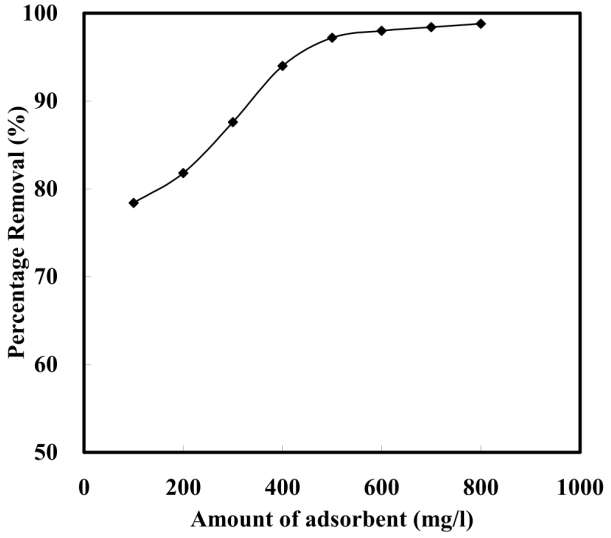

Fig. 3. Effect of adsorbent dosage on the percentage removal of MO by fly ash (pH 4, temperature = 303 K, t = 6 h, [MO] = 500 mgL^{-1}).

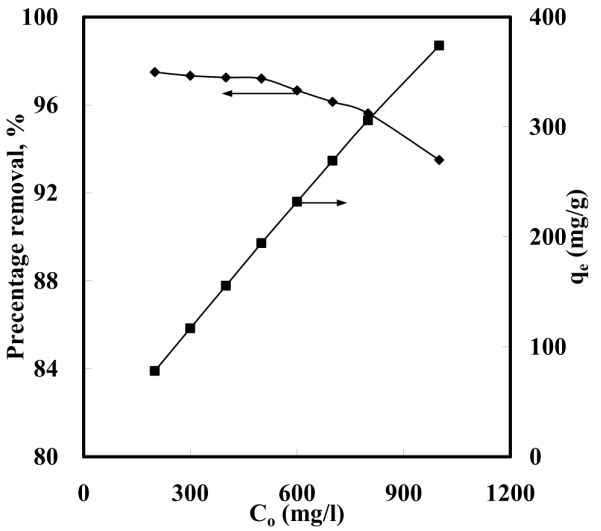

Fig. 4. Effect of initial dye concentration on the percentage removal of MO and equilibrium concentration by fly ash (pH 4, temperature = 303 K, t = 6 h, fly ash dosage = 500 mgL^{-1}).

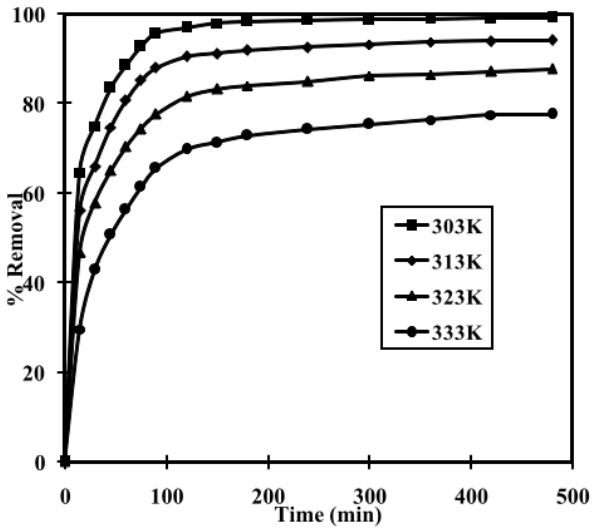

Fig. 5. Effect of contact time on the removal of MO by fly ash at different temperatures ([MO] = fly ash dosage = 500 mgL^{-1}, pH 4).

the aqueous and solid phases. The dosage increasing also enhanced the interaction between MO and fly ash. Therefore, the adsorption of MO increased.

3.4. Effect of contact time

Effect of contact time for removal of MO at a fixed concentration 500 mgL^{-1} by fly ash was studied in order to determine the equilibration time for maximum adsorption at different temperatures. The results indicated that the rate of MO removal progressively decreases with time. Nearly 5 h was required to reach the equilibrium adsorption for all the temperatures. Therefore, the equilibration time was set conservatively to 6 h for further experiments. Fig. 5 shows that the adsorption rate was very fast initially. 50% of adsorption for all the temperatures was taken in less than 60 min and gradually tails off thereafter. The removal curves were single, smooth and continuous indicating monolayer coverage of dye on the outer surface of adsorbent.

3.5. Adsorption kinetics study

In order to investigate the adsorption processes of MO by fly ash at different temperatures, pseudo-first-order, pseudo-second-order and intra-particle diffusion kinetic models were used.

3.5.1. Pseudo first order model

A simple kinetic analysis of adsorption is the Lagergren or pseudo first-order Eq. (2):

$$\frac{dq_t}{dt} = k_1\left(q_e - q_t\right) \tag{2}$$

where q_t is the amount of adsorbate adsorbed at time t (mgg^{-1}), q_e is the adsorption capacity at equilibrium (mgg^{-1}), k_1 is the pseudo-first-order rate constant (min^{-1}), and t is the contact time (min). After definite integration, by applying the initial conditions $q_t = 0$ at $t = 0$ and $q_t = q_t$ at $t = t$, Eq. (2) becomes [23,24]:

$$\ln\left(q_e - q_t\right) = \ln q_e - k_1 t \tag{3}$$

The rate constant, k_1 is obtained from slope of the linear plots of $\log(q_e - q_t)$ vs. t. For different temperatures, k_1 obtained for adsorption over 6 h are given in Table 2 along with the corresponding correlation coefficients.

3.5.2. Pseudo second order model

In addition, a pseudo-second-order [25] based on adsorption equilibrium capacity may be expressed as Eq. (4)

$$\frac{dq_t}{dt} = k_2\left(q_e - q_t\right)^2 \tag{4}$$

where k_2 is the pseudo-second-order rate constant (gmg^{-1}min^{-1}). Integrating Eq. (4) and applying the initial conditions $t = 0$ and $q_t = 0$ to $t = t$ and $q_e = q_t$, the following Eq. (5) is obtained:

$$\frac{t}{q_t} = \frac{1}{k_2 q_e^2} + \frac{t}{q_e} \tag{5}$$

The initial sorption rate, h (mgg^{-1}min^{-1}), at t = 0 is defined as:

$$h = k_2 q_e^2 \tag{6}$$

Fig. 6 shows the plot of t/q_t vs. t. The equilibrium adsorption capacity, q_e is obtained from the slope of the

Table 2
Kinetic parameters for the removal of MO by fly ash at different temperatures ([MO] = fly ash dosage = 500 mgL^{-1}, pH 4)

Temp. (K)	Pseudo-first-order model				Pseudo-second-order model				Intra-particle diffusion model					
	$q_{e,exp}$ (mgg^{-1})	$q_{e,cal}$ (mgg^{-1})	k_f (min^{-1})	R^2	$q_{e,cal}$ (mgg^{-1})	h ($mg(gmin)^{-1}$)	$k_s \times 10^4$ ($g(mgmin)^{-1}$)	R^2	$k_{id,1}$ ($mg/g\ min^{1/2}$)	I_1 (mgg^{-1})	R^2	$k_{id,2}$ ($mg/g\ min^{1/2}$)	I_2 (mgg^{-1})	R^2
303	198.48	49.52	0.0324	0.8831	202.11	28.25	6.92	0.9998	11.2032	88.45	0.9875	0.3307	191.65	0.8054
313	188.40	65.51	0.0294	0.9330	193.08	18.17	4.87	0.9998	11.6836	68.55	0.9907	0.6699	174.42	0.9610
323	175.60	70.30	0.0236	0.9242	181.12	11.69	3.56	0.9999	10.9815	53.87	0.9889	1.0472	153.25	0.9588
333	155.36	94.77	0.0272	0.9504	163.98	6.56	2.44	0.9998	12.6168	14.07	0.9893	1.4301	125.45	0.9663

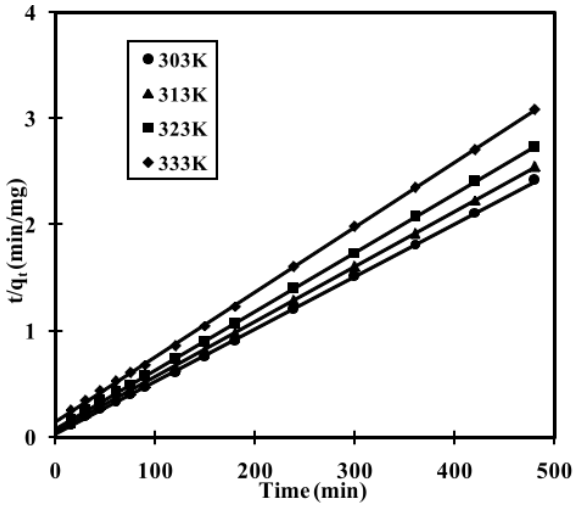

Fig. 6. Pseudo-second-order kinetic plot for the removal of MO by fly ash at different temperatures ([MO] = fly ash dosage = 500 mgL^{-1}, pH 4).

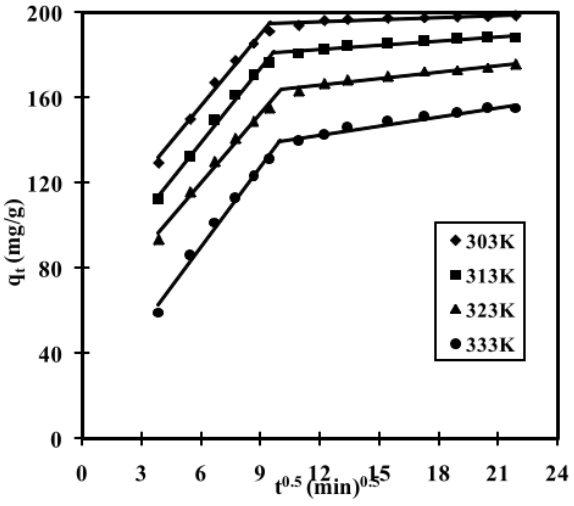

Fig. 7. Plots of amount of dye adsorbed (q_t) vs. $t^{0.5}$ for evaluating intra particle diffusion of MO at different temperatures ([MO] = fly ash dosage = 500 mgL^{-1}, pH 4).

plot and the initial sorption rate h is obtained from the intercept. Since q_e is known from the slope, the pseudo-second-order constant k_2 can be determined from the value of the initial sorption rate. The values of h, q_e and k_2 along with correlation coefficients for pseudo-second-order model are given in Table 2. The $q_{e,exp}$ and $q_{e,cal}$ values for the pseudo-first-order and pseudo-second-order models are also given in Table 2. The $q_{e,exp}$ and $q_{e,cal}$ values are very close to each other from pseudo-second-order model.

3.5.3. Intra particle diffusion

The possibility of intra-particle diffusion was explored by using the intra-particle diffusion model

$$q_t = k_{id} t^{1/2} + I \tag{7}$$

where k_{id} is the intra-particle diffusion rate constant (mg g^{-1} min$^{-1/2}$) and I is the intercept (mg g^{-1}). According to Eq. (7), a plot of q_t vs. $t^{1/2}$ should be a straight line with a slope k_{id} and intercept I when adsorption mechanism follows the intra-particle diffusion process. Fig. 7 presents a plot of q_t vs. $t^{1/2}$ for the adsorption of MO by fly ash. From Fig. 7 it may be seen that there are two separate regions viz., the initial portion is attributed to the bulk diffusion and the linear portion to intra-particle diffusion [26]. The values of $k_{id,1}$ and $k_{id,2}$ as obtained from the slopes and I_1 and I_2 from intercepts of the two straight lines are listed in Table 2.

3.6. Adsorption equilibrium study

To optimize the design of system for the adsorption of adsorbates, it was important to establish the most appropriate correlation for the equilibrium curves. Various isotherm equations like Langmuir, Freundlich, Redlich–Peterson (R–P) and Temkin were used to describe the equilibrium characteristics of adsorption.

The Freundlich isotherm [27] was derived by assuming a heterogeneous surface with a non-uniform distribution of heat of adsorption over the surface. Whereas in the Langmuir [28] theory, the basic assumption was that the sorption takes place at specific homogeneous sites within the adsorbent.

The R–P isotherm [29] can be described as follows:

$$q_e = \frac{K_R C_e}{1 + a_R C_e^{\beta}} \tag{8}$$

where K_R is R–P isotherm constant (Lg^{-1}), a_R is R–P isotherm constant (Lmg^{-1}) and β is the exponent which lies between 0 and 1, C_e is the equilibrium liquid phase concentration (mgL^{-1}).

For high concentrations, Eq. (8) reduces to Freundlich isotherm

$$q_e = K_F C_e^{1/n} \tag{9}$$

where $K_F = K_R/a_R$ is the Freundlich constant (Lmg^{-1}), and $1/n = (1 - \beta)$ is the heterogeneity factor. For β = 1, Eq. (8) reduces to Langmuir equation, i.e.

$$q_e = \frac{q_m K_L C_e}{1 + K_L C_e} \tag{10}$$

where K_L (= a_R) is the Langmuir adsorption constant (Lmg^{-1}) related to the energy of adsorption and q_m (= K_R/a_R) signifies adsorption capacity (mgg^{-1}).

For β = 0, Eq. (8) reduces to Henry's equation, i.e.

$$q_e = \frac{K_R C_e}{1 + a_R} \tag{11}$$

The R–P isotherm incorporates three parameters and can be applied in either a homogenous or a heterogeneous system. Eq. (8) can be converted to a linear form by taking logarithms of both the sides as:

$$\ln\left(K_R\frac{C_e}{q_e}-1\right)=\ln a_R+\beta\ln C_e \tag{12}$$

A minimization procedure has been adopted to solve Eq. (12) by maximizing the correlation coefficient between the predicted values of q_e from Eq. (12).

The Temkin isotherm

$$q_e=\frac{RT}{b}\ln\left(K_T C_e\right) \tag{13}$$

can be linearized as:

$$q_e=B_1\ln K_T+B_1\ln C_e \tag{14}$$

where

$$B_1=\frac{RT}{b}$$

Temkin isotherm contains a factor that explicitly takes into account the adsorbate-adsorbent interactions. This isotherm assumes that (i) the heat of adsorption of all the molecules in the layer decreases linearly with coverage due to adsorbent-adsorbate interactions, and that (ii) the adsorption is characterized by a uniform distribution of binding energies, up to some maximum binding energy [30,31]. A plot of q_e vs. ln C_e enables the determination of the isotherm constants B_1 and K_T from the slope and the intercept, respectively. K_T is the equilibrium binding constant (Lmg^{-1}) corresponding to the maximum binding energy and constant B_1 is related to the heat of adsorption.

Another equation used for the analysis of isotherms was proposed by Dubinin and Radushkevich (D–R) [32]. The D–R isotherm assumes no homogeneous surface of the adsorbent. The D–R equation can be expressed as

$$q_e=q_s\exp\left(-B\varepsilon^2\right) \tag{15}$$

where q_s is the D–R constant and ε can be correlated as:

$$\varepsilon=RT\ln\left(1+\frac{1}{C_e}\right) \tag{16}$$

The constant B gives the mean free energy E of sorption per molecule of sorbate. When it is transferred to the surface of the solid from infinity in the solution and can be computed using the following relationship [33]:

$$E=\frac{1}{\sqrt{2B}}$$

Freundlich, Langmuir, R–P, Temkin and D–R isotherm constants are determined from the plots of ln q_e vs. ln C_e, C_e/q_e vs. C_e (Fig. 8), ln ($K_R C_e/q_e$ – 1) vs. ln C_e (Fig. 9), q_e vs. ln C_e (Fig. 10), and ln q_e ν ε^2, respectively, at 303, 313, 323 and 333 K.

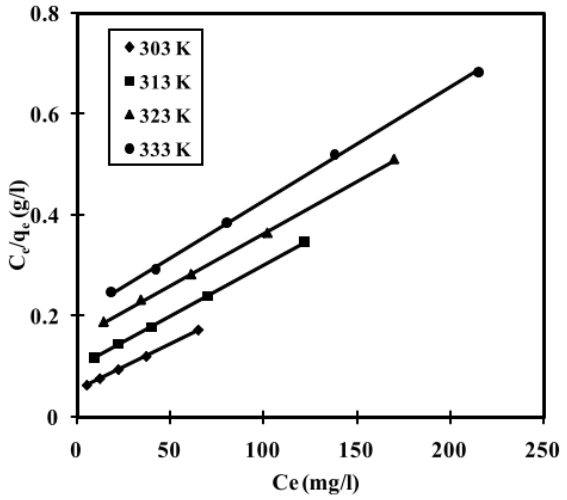

Fig. 8. Langmuir isotherm plots for the removal of MO at different temperatures ([MO] = fly ash dosage = 500 mgL^{-1}, pH 4, t = 6 h).

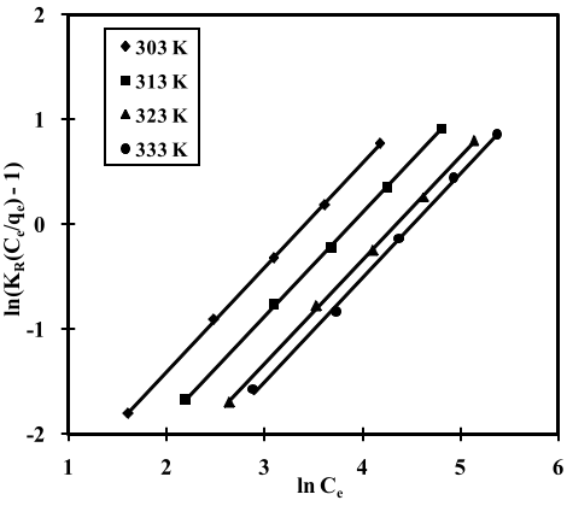

Fig. 9. Redlich–Peterson isotherm plots for the removal of MO at different temperatures ([MO] = fly ash dosage = 500 mgL^{-1}, pH 4, t = 6 h).

Fig. 11 shows a comparison of the above mentioned adsorption isotherms and experimental results. The model parameters of all isotherms obtained from nonlinear regression are presented in Table 3. As seen the R_1^2 value of Langmuir and R–P isotherm is higher when compared to the correlation coefficients value of Freundlich and the Temkin isotherms. Hence both Langmuir and R–P are the best fit isotherms to represent the experimental data of MO onto fly ash.

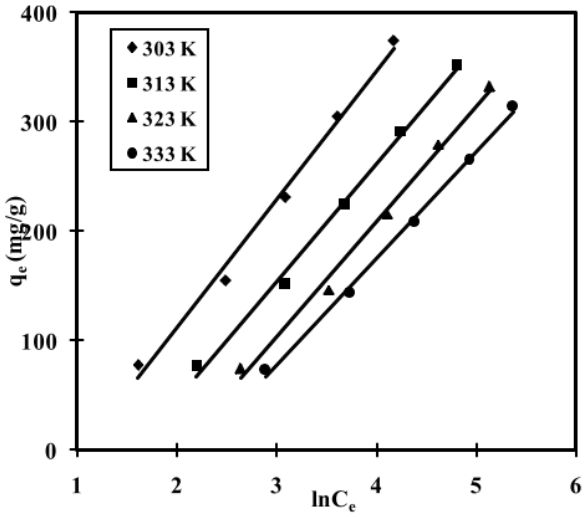

Fig. 10. Temkin isotherm plots for the removal of MO at different temperatures ([MO] = fly ash dosage = 500 mgL^{-1}, pH 4, t = 6 h).

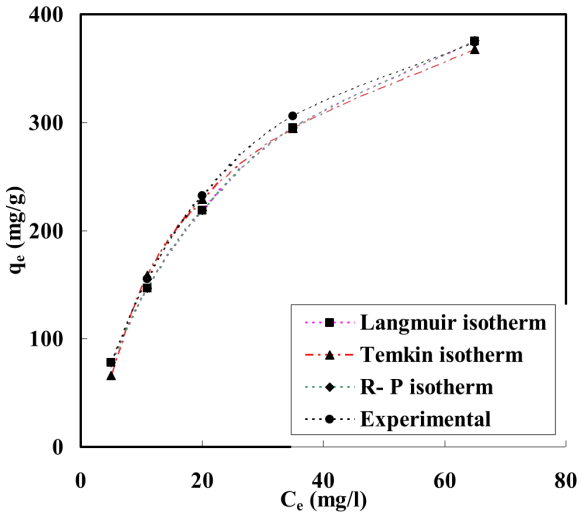

Fig. 11. Comparison of different isotherms for adsorption of MO by fly ash ([MO] = fly ash dosage = 500 mgL^{-1}, pH 4, t = 6 h).

3.7. Error analysis

Due to the inherent bias resulting from linearisation, different error functions of non-linear regression basin were employed in this study to find out the best-fit isotherm model to the experimental equilibrium data.

3.7.1. The sum of the squares of the errors (SSE)

This error function, SSE, is given as:

$$\text{SEE} = \sum_{i=1}^{n} \left(q_{e,cal} - q_{e,\exp}\right)_i^2 \tag{17}$$

Here, $q_{e,cal}$ and $q_{e,\exp}$ are the calculated and the experimental value of the equilibrium adsorbate solid concentration in the solid phase (mgg^{-1}) respectively and n is the number of data points. This most commonly used error function, SSE, has one major drawback that it will result in the calculated isotherm parameters providing a better fit at the higher end of the liquid phase concentration range. This is because of the magnitude of the errors, which increase as the concentration increases.

3.7.2. The sum of the absolute errors (SAE)

SAE is given as:

$$\text{SAE} = \sum_{i=1}^{n} \left|q_{e,cal} - q_{e,\exp}\right|_i \tag{18}$$

The isotherm parameters determined by this method provide a better fit as the magnitude of the errors increase, biasing the fit towards the high concentration data.

3.7.3. The average relative error (ARE) [34]

ARE is given as:

$$\text{ARE} = \frac{100}{n} \sum_{i=1}^{n} \left|\frac{q_{e,\exp} - q_{e,cal}}{q_{e.\exp}}\right|_i \tag{19}$$

This error function attempts to minimize the fractional error distribution across the entire concentration range.

3.7.4. The hybrid fractional error function (HYBRID)

HYBRID is given as:

$$\text{HYBRID} = \frac{100}{n-p} \sum_{i=1}^{n} \left[\frac{q_{e,\exp} - q_{e,cal}}{q_{e,\exp}}\right]_i \tag{20}$$

This error function was developed [35] to improve the fit of the ARE method at low concentration values. Instead of n as used in ARE, the sum of the fractional errors was divided by $(n - p)$, where p is the number of parameters in the isotherm equation.

3.7.5. Marquardt's percent standard deviation (MPSD)

MPSD [36] was used by a number of researchers in the field [16,17,37] to test the adequacy and accuracy of the model fit with the experimental data. It has somewhat similarity to the geometric mean error distribution, but modified by incorporating the number of degrees of freedom. This error function is given as:

$$\text{MPSD} = 100 \sqrt{\frac{1}{n-p} \sum_{i=1}^{n} \left[\frac{q_{e.\exp} - q_{e,cal}}{q_{e,\exp}}\right]_i^2} \tag{21}$$

Table 3
Isotherm parameters for the removal of MO by fly ash at different temperatures (t = 6 h, [MO] = 50–300 mgL^{-1}, fly ash dosage = 500 mgL^{-1})

Freundlich constants				
T (K)	K_F ((mg/g)/(mg/l)$^{1/n}$)	1/n	R_1^2 (linear)	R_1^2 (non-linear)
303	31.4369	0.6179	0.9801	0.9551
313	22.8505	0.5912	0.9758	0.9660
323	16.2435	0.6073	0.9793	0.9671
333	14.6609	0.5863	0.9776	0.9824
Langmuir constants				
T (K)	K_L (mg^{-1})	q_m (mgg^{-1})	R_L	R_1^2 (linear)	R_1^2 (non-linear)
303	0.0331	549.4525	0.0570	0.9998	0.9972
313	0.0204	493.5975	0.0892	0.9997	0.9998
323	0.0132	484.8245	0.1336	0.9995	0.9994
333	0.009	444.6826	0.1539	0.9993	0.9991
R–P constants				
T (K)	K_R (g^{-1})	a_R (mg^{-1})$^{1/\beta}$	β	R_1^2 (linear)	R_1^2 (non-linear)
303	18.1826	0.0336	0.9957	0.9998	0.9970
313	10.0774	0.0214	0.9883	0.9996	0.9996
323	6.2903	0.0136	0.9889	0.9994	0.9992
333	4.8906	0.0115	0.9902	0.9982	0.9993
Temkin constants				
T (K)	K_T (mg^{-1})	B_1	R_1^2 (linear)	R_1^2 (non-linear)
303	0.3511	117.4436	0.9915	0.9971
313	0.2080	107.5583	0.9942	0.9942
323	0.1328	105.3611	0.9930	0.9965
333	0.1102	97.5209	0.9967	0.9935
D–R constants				
T (K)	q_s (mgg^{-1})	E ($kJmol^{-1}$)	R_1^2 (linear)	R_1^2 (non-linear)
303	283.0452	269.5676	0.8518	0.7950
313	268.4178	163.3994	0.8511	0.7583
323	256.8602	111.3696	0.8537	0.7847
333	246.6028	90.7804	0.8692	0.7678

The values of the error functions are presented in Table 4. By comparing the results of the values of the error functions, it was found that Langmuir model best fits the MO adsorption isotherm data for the fly ash at all temperatures. It may, however, be noted that the non-linear correlation coefficients, R^2 and the error analysis values are similar for the Langmuir and R–P isotherms. Hence Langmuir isotherms could be used for MO adsorption on fly ash.

3.8. Effect of temperature and thermodynamic parameters

The thermodynamic parameters obtained for the systems under investigation, using Eqs. (22), (23) and (24), are given in Table 5 [38].

$$\Delta G^o = -RT\ln K \tag{22}$$

$$\Delta H^o = -R\left(\frac{T_2T_1}{T_2 - T_1}\right)\ln\frac{K_1}{K_2} \tag{23}$$

$$\Delta S^o = \frac{\Delta H^o - \Delta G^o}{T} \tag{24}$$

The negative free energy values (Table 5) indicate the feasibility of the process and spontaneous nature of the adsorption. Free energy decreasing with increases in temperature indicating thereby, a decrease in adsorption at higher temperature. The negative values of enthalpy change for the process suggests the exothermic and physi-

Table 4
Values of five different error analyses of isotherm models for adsorption of MO by fly ash (t = 6 h, [MO] = 50–300 mgL^{-1}, fly ash dosage = 500 mgL^{-1})

Temperature (K)	Isotherm	SSE	SAE	ARE	HYBRID	MPSID
313	Freundlich	3546.7096	119.8925	10.4435	5.2091	13.7502
	Langmuir	379.0947	34.3597	3.0753	4.9280	5.1246
	Temkin	484.5745	36.1289	4.8165	6.7014	9.2311
	D–P	13156.0694	207.7780	17.2664	–0.7134	25.9408
	R–P	391.2463	35.5225	3.1770	4.9924	5.2161
323	Freundlich	2312.7678	88.4593	8.0523	–0.5978	11.0300
	Langmuir	11.2532	6.7144	0.6485	–0.0873	0.9571
	Temkin	275.3806	32.5218	4.7904	1.3704	8.3716
	D–P	12509.0061	206.1623	18.4646	–3.7746	28.7939
	R–P	19.3063	8.2381	0.6704	–0.0931	0.9932
333	Freundlich	2015.6572	86.1892	8.3371	1.1704	11.2442
	Langmuir	50.7562	13.5048	1.3726	1.8554	2.3011
	Temkin	150.8358	25.1842	3.9412	3.3647	7.4422
	D–P	9986.5466	184.3769	16.9387	–1.8486	25.8341
	R–P	65.6232	15.7965	1.5550	1.9486	2.5466
343	Freundlich	963.8703	53.4207	5.8019	–3.0425	8.5709
	Langmuir	91.7070	17.5097	1.7646	–2.6259	2.6406
	Temkin	320.1069	36.3928	4.8559	1.5105	7.3979
	D–P	9108.7650	177.5381	17.5566	–4.8856	27.4602
	R–P	97.5568	18.8482	1.8697	–2.7829	2.6411

Table 5
Thermodynamic parameters for adsorption of MO by fly ash (t = 6 h, [MO] = 50–300 mgL^{-1}, fly ash dosage = 500 mgL^{-1})

Temperature	$\Delta G°$ (kJ(molK) $^{-1}$)	$\Delta H°$ (kJ(mol K) $^{-1}$)	$\Delta S°$ (J(mol K)$^{-1}$)
303	–23.4042		
313	–22.9171	–38.1629	–48.7085
323	–22.4802	–37.4016	–46.1961
333	–22.1159	–36.415	–42.9426

cal nature. The establishment of firm bonding on the adsorbent will be facilitated when the adsorbate molecules reside on the adsorption sites for a longer time as their molecular geometry retards slipping off from the surface of the adsorbent [39]. The negative ΔS values obtained for the adsorption of MO by fly ash reflect that no significant change occurs in the internal structure of the adsorbent material during adsorption. The negative ΔS values were not uncommon in adsorption, and many researchers have also reported negative ΔS values [21,40]. Similar trend was observed for diazo and triphenylmethane dyes on rice bran-based activated carbon [41].

4. Conclusions

The result shows that the potential of coal fly ash a waste material, to be a low-cost sorbent for removing MO. Adsorption kinetics is best represented by a second-order rate expression at different temperatures. The Langmuir and Redlich–Peterson isotherms fit with the equilibrium adsorption data. Error analysis showed that the Langmuir isotherm is more suitable for adsorptive removal of MO on fly ash. The thermodynamic parameters were evaluated and the results show that adsorption process is spontaneous and exothermic in nature. Monolayer adsorption on fly ash is found to be effective for the removal of MO from aqueous solution.

References

[1] W. Chu, Dye removal from textile dye wastewater using recycled alum sludge, Wat. Res., 35 (2001) 3147.
[2] C.O. Neill, F.R. Hawkes, S.R.R. Esteves, D.L. Hawkes and S.J. Wilcox, Anaerobic and aerobic treatment of a simulated textile effluent, J. Chem. Tech. Biol., 74 (1999) 993.
[3] Y. Al-Degs, M.A.M Kharaisheh, S.J. Allen and M.N. Ahmad, Effect of carbon surface chemistry on the removal of reactive dyes from textile effluent, Wat. Res., 34 (2000) 927.
[4] M.M. Abd El-Latif and A.M. Ibrahim, Adsorption, kinetic and equilibrium studies on removal of basic dye from aqueous solutions using hydrolyzed oak sawdust, Desal. Wat. Treat., 6 (2009) 252.

[5] B.T. Tan, T.T. Teng and A.K.M. Omar, Removal of dyes and industrial dye wastes by magnesium chloride, Wat. Res., 34 (2000) 597.
[6] N. Zaghbani, A. Hafiane and M. Dhahbi, Removal of Direct Blue 71 from wastewater using micellar enhanced ultrafiltration, Desal. Wat. Treat., 6 (2009) 204.
[7] K.V. Radha, V. Sridevi and K. Kalaivani, Electrochemical oxidation for the treatment of textile industry wastewater, Bioresour. Technol., 100 (2009) 987.
[8] N.J.D Graham, C.C.S Brandao and P.F. Luckham, Evaluating the removal of color from water using direct-filtration and dual coagulants, J. AWWA, 84 (1992) 105.
[9] A.K. Mittal and C. Venkobachar, Sorption and desorption of dyes by sulfonated coal, J. Environ. Eng. Div., 119 (1993) 366.
[10] D. Sun, X. Zhang, Y. Wu and X. Liu, Adsorption of anionic dyes from aqueous solution on fly ash, J. Hazard. Mater., 181 (2010) 335.
[11] J.X. Lin, S.L. Zhan, M.H. Fang, X.Q. Qian and H. Yang, Adsorption of basic dye from aqueous solution onto fly ash, J. Environ. Manage., 87 (2008) 193.
[12] F. Ferrero, Dye removal by low cost adsorbents: Hazelnut shells in comparison with wood sawdust, J. Hazard. Mater., 142 (2007) 144.
[13] G. McKay and F. Allexander, Kinetics of the removal of basic dye from effluent using silica, Chem. Eng., 84 (1977) 234.
[14] A. Gurses, C. Dogar, M. Yalcin, M. Acikyildiz, R. Bayrak and S. Karaca, The adsorption kinetics of the cationic dye, methylene blue, onto clay, J. Hazard. Mater., 131 (2006) 217.
[15] M.S. El-Geundi, Color removal from textile effluents by adsorption technique, Wat. Res., 25 (1991) 271.
[16] I.D. Mall, V.C. Srivastava and N.K. Agarwal, Removal of orange-G and methyl violet dyes by adsorption onto bagasse fly ash e kinetic study and equilibrium isotherm analyses, Dyes Pigments, 69 (2006) 210.
[17] I.D. Mall, V.C. Srivastava, N.K. Agarwal and I.M. Mishra, Removal of Congo red from aqueous solution by bagasse fly ash and activated carbon: kinetic study and equilibrium isotherm analyses, Chemosphere, 61 (2005) 492.
[18] V.S. Mane, I.D. Mall and V.C. Srivastava, Use of bagasse fly ash as an adsorbent for the removal of brilliant green dye from aqueous solution, Dyes Pigments, 73 (2006) 269.
[19] S.D. Lambert and N.J.D. Graham, Adsorption methods for treating organically colored upland waters, Environ. Technol. Lett., 10 (1989) 785.
[20] W. Delee, C.O. Neill, F.R. Hawkes and H.M. Pinheiro, Anaerobic treatment of textile effluents: a review, J. Chem. Technol. Biotechnol., 73 (1998) 323.
[21] M. Matheswaran and T. Karunanithi, Adsorption of Chrysoidine R by using fly ash in batch process, J. Hazard. Mater., 145 (2007) 154.
[22] Z. Wu, I.S. Ahn, C.H. Lee, J.H. Kim, Y.G. Shul and K. Lee, Enhancing the organic dye adsorption on porous xerogels, Colloids Surfaces A: Physicochem. Eng. Aspects, 240 (2004) 157.
[23] S. Lagergren, About the theory of so-called adsorption of soluble substances, Ksver Veterskapsakad Handl, 24 (1898) 1.
[24] K.R. Hall, L.C. Eagleton, A. Acrivos and T. Vermeulen, Pore and solid diffusion kinetics in fixed bed adsorption under constant pattern conditions, Ind. Eng. Chem. Fund, 5 (1966) 212.
[25] Y.S. Ho and G. McKay, Pseudo-second order model for sorption processes, Process Biochem., 34 (1999) 451.
[26] S.J. Allen, G. McKay and K.Y.H Khader, Intraparticle diffusion of a basic dye during adsorption onto sphagnum peat, Environ. Pollut., 56 (1989) 39.
[27] H.M.F. Freundlich, Over the adsorption in solution, J. Phys. Chem., 57 (1906) 385.
[28] I. Langmuir, Adsorption of gases on plane surface of glass, mica and platinum, J. Am. Chem. Soc., 40 (1918) 1361.
[29] O. Redlich and D.L. Peterson, A useful adsorption isotherm, J. Phys. Chem., 63 (1959) 1024.
[30] M.J. Temkin and V. Pyzhev, Kinetics of ammonia synthesis on promoted iron catalysts, Acta Physiochim. URSS, 12 (1940) 217.
[31] Y. Kim, C. Kim, I. Choi and S. Rengraj, Arsenic removal using mesoporous alumina prepared via a templating method, Environ. Sci. Technol., 38 (2004) 924.
[32] M.M. Dubinin and L.V. Radushkevich, Equation of the characteristic curve of activated charcoal, Proc. Acad. Sci. USSR, 55 (1947) 327.
[33] S.M. Hasany and M.H. Chaudhary, Sorption potential of Hare river sand for the removal of antimony from acidic aqueous solution, Appl. Radiat. Isot., 47 (1996) 467.
[34] A. Kapoor and R.T. Yang, Correlation of equilibrium adsorption data of condensable vapours on porous adsorbents, Gas. Separ. Purif., 3 (1989) 187.
[35] J.F. Porter, G. McKay and K.H. Choy, The prediction of sorption from a binary mixture of acidic dyes using single- and mixed isotherm variants of the ideal adsorbed solute theory, Chem. Eng. Sci., 54 (1999) 5863.
[36] D.W. Marquardt, An algorithm for least-squares estimation of nonlinear parameters, J. Soc. Ind. Appl. Math., 11 (1963) 431.
[37] J.C.Y. Ng, W.H. Cheung and G. McKay, Equilibrium studies for the sorption of lead from effluents using chitosan, Chemosphere, 52 (2003) 1021.
[38] Y.C. Sharma, G. Prasad and D.C. Rupainwar, Adsorption for the removal of Cd(II) from effluents, Int. J. Environ. Stud., 37 (1991) 183.
[39] S.J. Allen, G. McKay and K.Y.H. Khuder, Equilibrium adsorption isotherms of basic dyes onto lignite, J. Chem. Technol. Biotechnol., 45 (1989) 291.
[40] K.P. Singh, D. Mohan, S. Sinha, G.S. Tondon and D. Gosh, Color removal from wastewater using low-cost activated carbon derived from agricultural waste material, Ind. Eng. Chem. Res., 42 (2003) 1965.
[41] M. Sankar, G. Sekaran, S. Sadulla and T. Ramasami, Removal of diazo and triphenylmethane dyes from aqueous solutions through an adsorption process, J. Chem. Technol. Biotechnol., 74 (1999) 337.